Silicon Nanocrystals at Elevated Temperatures: Retention of Photoluminescence and Diamond Silicon to β-Silicon Carbide Phase Transition

Clare E. Rowland,[†] Daniel C. Hannah,[†] Arnaud Demortière,[‡,§] Jihua Yang,[⊥] Russell E. Cook,[‡] Vitali B. Prakapenka,[∥] Uwe Kortshagen,[⊥] and Richard D. Schaller[†,#,*]

[†]Department of Chemistry, Northwestern University, Evanston, Illinois 60208, United States, [‡]Electron Microscopy Center, Argonne National Laboratory, Argonne, Illinois 60439, United States, [§]Department of Physics, Illinois Institute of Technology, Chicago, Illinois 60616, United States, [⊥]Department of Mechanical Engineering, University of Minnesota, Minneapolis, Minnesota 55455, United States, [∥]Center for Advanced Radiation Sources, University of Chicago, Chicago, Illinois 60637, United States, and [#]Center for Nanoscale Materials, Argonne National Laboratory, Argonne, Illinois 60439, United States

ABSTRACT We report the photoluminescence (PL) properties of colloidal Si nanocrystals (NCs) up to 800 K and observe PL retention on par with core/shell structures of other compositions. These alkane-terminated Si NCs even emit at temperatures well above previously reported melting points for oxide-embedded particles. Using selected area electron diffraction (SAED), powder X-ray diffraction (XRD), liquid drop theory, and molecular dynamics (MD) simulations, we show that melting does not play a role at the temperatures explored experimentally in PL, and we observe a phase change to β-SiC in the presence of an electron beam. Loss of diffraction peaks (melting) with recovery of diamond-phase silicon upon cooling is observed under inert atmosphere by XRD. We further show that surface passivation by covalently bound ligands endures the experimental temperatures. These findings point to covalently bound organic ligands as a route to the development of NCs for use in high temperature applications, including concentrated solar cells and electrical lighting.

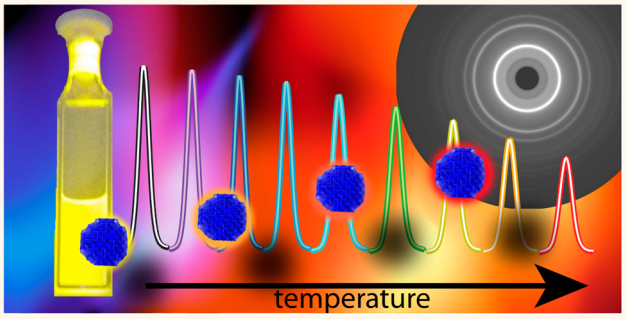

KEYWORDS: silicon · nanocrystals · photoluminescence · high temperature · phase transition

Interest in the photophysical properties of semiconductor nanocrystals (NCs) arises from well-known particle-size controlled bandgap, high photoluminescence (PL) quantum yields, and facile processing for use in devices.[1−5] A number of applications subject NCs to elevated operating temperatures, including concentrated solar cells,[6] high brightness/current light-emitting diodes (LEDs),[7] and lasers.[8] However, PL quenching (and thus exciton quenching) is known to occur at elevated temperature,[9−14] which suggests deterioration of performance in such devices. Our prior examinations of CdSe and InP NCs point to electron and hole trapping as culprits for PL quenching with temperature elevation, while replacement of native ligands with a wide bandgap shell (ZnS) or inorganic capping ligand (S^{2-}) has led to improved PL retention.[10,11] Despite the importance of the NC surface to high temperature PL performance, a key surface motif remains unexplored, namely the covalently bound organic ligand. In most core-only NC compositions, the surface is passivated by an ionically bound ligand (*e.g.*, trioctylphosphine on CdSe), the volatility and departure of which likely drives the formation of trap states at lower coordination surface atoms.[15] By contrast, silicon NCs can form covalent bonds with carbon,[16,17] the stability of which may lead to a more thermally robust surface passivation.

* Address correspondence to schaller@northwestern.edu, schaller@anl.gov.

Received for review June 2, 2014 and accepted September 2, 2014.

Published online September 02, 2014
10.1021/nn5029967

Also critical to the useful operational range of a photoactive material is the well-known melting temperature (T_m) reduction exhibited by nanosized particles relative to the bulk composition.[18−20] Depending nonlinearly on particle size, few nanometer diameter NCs can melt at hundreds of degrees Kelvin below the bulk-phase, $T_{m,bulk}$, owing to their large surface/volume ratio. For instance, silicon NCs with diameters of 2 and 4 nm are reported to melt at respective temperatures of $0.3T_{m,bulk}$ and $0.6T_{m,bulk}$, where $T_{m,bulk}$ = 1687 K.[18] Furthermore, irreversible effects active even below T_m, such as sintering, can irreversibly alter the particles and degrade PL.

Here we report studies of Si NC thermal stability and show that organically capped Si NCs retain PL in similarity to CdSe/ZnS and InP/ZnS core/shell compositions up to 800 K. We demonstrate robust PL recovery upon return to near-ambient conditions, and molecular dynamics (MD) simulations confirm the retention of covalently bound ligands throughout this temperature range. We further corroborate the apparent physical stability of the colloidally prepared NCs at temperatures well beyond previously reported T_m for physically synthesized particles using transmission electron microscopy (TEM), selected area electron diffraction (SAED), and powder X-ray diffraction (XRD), as well as through theoretical modeling and MD simulations.

RESULTS AND DISCUSSION

Figure 1 shows time-integrated PL spectra and time-resolved PL (trPL) decays collected from drop-cast films of Si NCs synthesized by plasma dissociation of SiH_4 gas and passivated by reaction with dodecene (see Materials and Methods).[17] Samples were excited using a 35 ps 405 nm pulsed diode laser. With increases

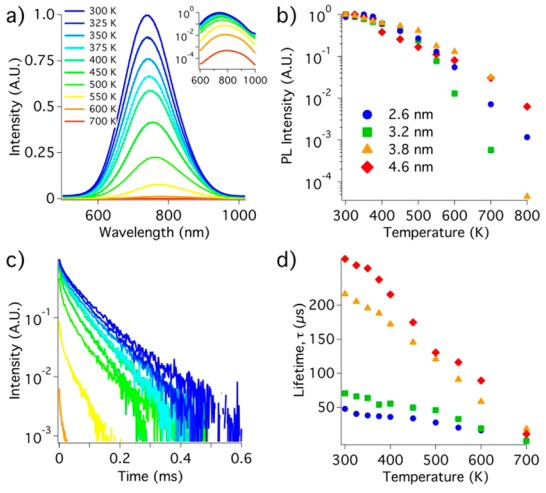

Figure 1. Spectra of Si NCs collected from drop-cast films heated in an evacuated optical oven are here normalized to the intensity of the 300 K spectrum. (a) Static PL falls off with increasing temperature in a 3.2 nm diameter sample and (b) in integrated static PL in all four samples. (c) Time-resolved PL decays likewise decrease with increasing temperature in the 3.2 nm Si sample, (d) a trend further reflected in decreasing excited state lifetimes with increasing temperature in all samples.

of temperature over the range studied (300−800 K), static PL intensity decreases by 1−2 orders of magnitude by 600 K and 2−4 orders of magnitude by 800 K for all four samples, exhibiting no distinct size dependence. The observed changes in PL intensity are comparable to those observed in compositions with a wide bandgap inorganic shell (*e.g.*, CdSe/ZnS, InP/ZnS, InP/S^{2-}), while other examples of ligand-terminated cores exhibit markedly lower PL thermal stability.[10−12,21] Worth mention, decreases in temperature below ambient for both core/shell and organically passivated cores (including Si NCs) are known to yield increases in PL intensity.[22−24] trPL dynamics collected at the emission maximum indicate a decrease in excited state lifetime, τ, with increasing temperature as determined by fitting time-resolved PL traces using a single exponential function (see Supporting Information for examinations of longer term PL stability at sustained elevated temperatures).

Effects such as reduced surface passivation and sintering can yield irreversible PL loss by eliminating emissive particles in the ensemble. We performed cyclical heating experiments to deconvolute such effects from reversible PL loss.[10,11] Figure 2 shows integrated PL of Si NCs obtained from a cyclical heating experiment (PL decay times in Supporting Information). Remarkably, PL loss and changes in τ are almost entirely reversible in all four Si samples up to 650 K. Only after heating to 800 K do irreversible effects become significant. These results are particularly surprising given experimental and theoretical T_m depression in Si NCs, where particles 2−4 nm in diameter have been reported to melt as low as 400−550 K.[18−20,25]

Irreversible processes such as Ostwald ripening and sintering, which can occur below T_m, may alter ensemble PL wavelength or fwhm upon cooling. We, however, find PL fwhm and energies, which, respectively, broaden and red-shift while at elevated temperature in correspondence with the Varshni effect,[26] reliably recover to initial values upon returning to 300 K (see Supporting Information, Figures S2−S4). Thus, if physical changes do occur in the NCs at elevated temperature, those NCs cease to emit; and on the basis of the recovery in PL intensity in cyclical heating experiments, the newly "darkened" ensemble represents a small fraction of the initially emitting NCs.

Theoretical considerations support the notion that Si crystallinity and surface passivation persists well beyond 800 K for the NC sizes considered here. First, a liquid drop model of NC melting based on classical thermodynamics and cohesive energies between surface atoms, including a correction to accommodate underestimation of T_m in covalently bonded materials, predicts T_m by eq 1,[27,28]

$$T_m(n) = T_m(\infty)\left[1-\left(\frac{1}{n}\right)^2\right] \quad (1)$$

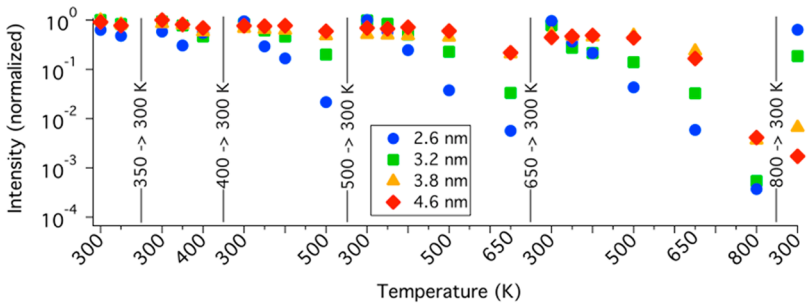

Figure 2. Normalized PL intensity measured during cyclical heating experiments decreases with increasing temperature but shows significant recovery upon return to near-ambient temperature, especially in the smaller, bluer-emitting samples.

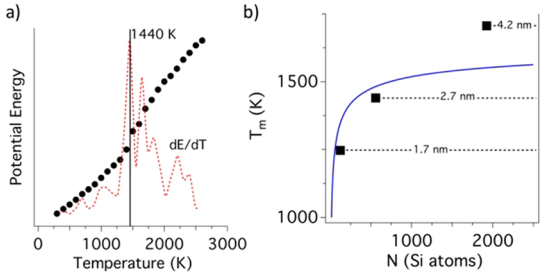

Figure 3. (a) Average potential energy *vs* temperature for a 2.6 nm-diameter, H-passivated Si NC. The data points represent an average of 2 ps of simulation of an equilibrated NC at the given temperature. The dashed line indicates the first derivative of the potential energy *vs* temperature. (b) Melting point as a function of Si NC temperature *via* multiple methods. The solid line indicates the prediction of the modified liquid drop model, while the square data points indicate first derivative maxima indicating melting temperatures from MD simulations.

where $n^3 = N$, and N is the number of Si atoms. Predictions based on the modified liquid drop model yield T_m from 1230 to 1553 K for NC sizes ranging from four-atom clusters to a 4 nm diameter Si NCs, respectively. Although this model predicts NC T_m size dependence, it does not account for atomistic details such as covalent surface chemistry, which may significantly impact thermal stability and T_m.

We use MD simulations to gain atomistic insight into the temperature-dependent behavior of Si NCs. Faceted Si NCs were created using the Wulff construction and experimentally known surface energies.[29] For simplicity and computational tractability, Si NC surfaces were passivated with hydrogen atoms (additional calculation details are available in the Supporting Information).[30−32] Figure 3a displays the potential energy of a 2.6 nm Si NC (558 atoms) at each temperature step, averaged over the 2 ps production run. A discontinuity, emphasized in the first derivative, is evident at 1440 K and indicates a solid−liquid transition (T_m,) that is depressed relative to $T_{m,bulk} = 1687$ K.[18] By similarly treating both a smaller and larger Si NC, a positive correlation appears between size and T_m, consistent with thermodynamic considerations (see Figure 3b and Supporting Information Figure S5). The MD simulations qualitatively agree with the modified liquid drop model and with prior MD studies employing the Stillinger-Weber potential,[33] although in the MD simulation T_m of the largest NC size approaches the experimentally determined $T_{m,bulk}$, perhaps because the interaction potential knowingly overestimates $T_{m,bulk}$.[34] Regardless, both methods predict that NC T_m values exceed the temperatures examined for PL.

MD simulations also suggest that Si−H bonds are stable over the PL measurement temperature range. Like the Si−C bond, the Si−H bond is covalent, and both exhibit a similar dissociation energy, D (D_{Si-H} = 91.8 kcal/mol, D_{Si-C} = 89.6 kcal/mol), the comparison of which serves as a simplified means to conceptualize the bond character.[35,36] The reactive bond-order potential used here is parametrized to capture bond-making and breaking,[30] yet MD does not exhibit ligand desorption until temperatures in excess of 1600 K. While further investigation is necessary to model this process with still higher accuracy, we note that, in aggregate, the similar dissociations of Si−C and Si−H bonds, coupled with the thermal stability found in MD simulations, support the notion advanced by the PL data presented here: namely, the covalently passivated Si NC surface exhibits enhanced thermal stability in comparison to the ionically bound organic ligands of InP and CdSe NCs.

Finally, to ascertain the size-dependent trends, we investigated T_m using TEM, SAED, and XRD. In support of the optical and theoretical data, SAED experiments reveal no melting at temperatures as high as 1000 K in either end-member of the studied Si NC sizes, and analysis of the size distribution in the 3.2 nm particles shows little sintering after heating to 800 K, with more pronounced sintering after heating to 1100 K (Figure 4, and Supporting Information Figures S6 and S7). SAED, however, indicates continued crystallinity at elevated temperatures. Rather than loss of order (melting), we observe a chemical phase transition to a new crystalline phase identified as β-SiC that replaces the original diamond crystal phase and persists upon returning to 300 K. In other systems, the ability to synthesize β-SiC relies on exploiting the same phase change that we observe here, with even bulk Si suitable as a starting material.[37] We find a size-dependent trend, with the

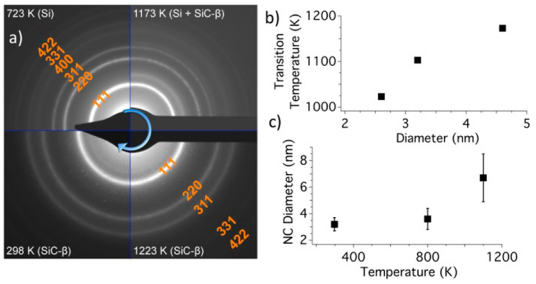

Figure 4. (a) Electron diffraction patterns during collected before, during, and after temperature ramping show a Si to β-SiC phase transition. (b) The phase transition temperature shows size dependence. (c) Size distribution analysis shows little change at 800 K, although effects of sintering become pronounced by 1100 K.

smallest NCs undergoing the phase transition at the lowest temperature, suggesting that melting may mechanistically facilitate the observed phase change. In support of this hypothesis, XRD reveals melting of the largest sample through the temperature-dependent loss of Bragg peaks (see Supporting Information, Figure S8), with near complete disappearance of diffraction coinciding with the phase change temperature observed in SAED. Even upon cooling and recrystallization, however, no evidence of SiC formation is observed, suggesting that the electron beam in SAED may facilitate the reactive phase transformation process or that differences between the vacuum conditions of SAED and inert atmosphere (Ar/H_2) of XRD may affect the chemistry taking place. Further investigation to deduce the subtleties of each technique notwithstanding, a degradation of structural integrity of the Si NCs at temperatures well above those often noted is evident.

CONCLUSIONS

The PL of Si NCs exhibits both persistence to high temperatures and resilience to thermal cycling akin to core/shell motifs. We suggest that the robustness of the surface passivation, arising from the covalency of the NC-ligand bond, aids PL retention, a point supported by the presented MD simulations. Moreover, while a report examining oxide-terminated Si suggests that melting might occur even well below 800 K for similarly size particles, our experimental and theoretical investigations point instead to higher melting temperatures at least for covalently passivated particles.

MATERIALS AND METHODS

Si NCs were synthesized by room temperature plasma dissociation of SiH_4 gas, using an H_2 flow in order to H-terminate Si NCs. Surface functionalization yielding covalently bound dodecane was accomplished by ultrasonicating and heating in a mixture of dodecene and mesitylene.[17] The samples are labeled here according to particle diameters, 2.6, 3.2, 3.8, and 4.6 nm, which correspond to ambient temperature maximum PL wavelengths of 670, 740, 880, and 890 nm, respectively.[38] Complete synthetic details are available in the Supporting Information.

Photoluminescence experiments were carried out on films drop-cast from toluene onto glass slides, which were mounted in an evacuated optical oven. Time-integrated and time-resolved PL were collected from samples photoexcited by a 35 ps, 405 nm pulsed diode laser using a thermoelectrically cooled CCD and avalanche photodiode, respectively. Additional experimental details are available in the Supporting Information.

Conflict of Interest: The authors declare no competing financial interest.

Supporting Information Available: Synthetic and experimental details; PL decay data and lifetimes, emission maxima, and fwhm of spectra collected during cyclical and linear heating experiments; SAED patterns; STEM images; XRD patterns. This material is available free of charge *via* the Internet at http://pubs.acs.org.

Acknowledgment. Use of the Center for Nanoscale Materials was supported by the U.S. Department of Energy, Office of Science, Office of Basic Energy Sciences, under Contract No. DE-AC02-06CH11357. XRD was performed at GeoSoilEnviroCARS (Sector 13), Advanced Photon Source, Argonne National Laboratory. GSECARS is supported by the National Science Foundation (EAR-1128799) and Department of Energy (DE-FG02-94ER14466). C.E.R. and D.C.H. acknowledge support by National Science Foundation Graduate Research Fellowships under Grant No. DGE-0824162. J.Y. and U.K. acknowledge support by the DOE Energy Frontier Research Center for Advanced Solar Photophysics.

REFERENCES AND NOTES

1. Hines, M. A.; Guyot-Sionnest, P. Synthesis and Characterization of Strongly Luminescing ZnS-Capped CdSe Nanocrystals. *J. Phys. Chem.* **1996**, *100*, 468–471.
2. Murray, C.; Norris, D. J.; Bawendi, M. G. Synthesis and Characterization of Nearly Monodisperse CdE (E = Sulfur, Selenium, Tellurium) Semiconductor Nanocrystallites. *J. Am. Chem. Soc.* **1993**, *115*, 8706–8715.
3. Luther, J. M.; Law, M.; Beard, M. C.; Song, Q.; Reese, M. O.; Ellingson, R. J.; Nozik, A. J. Schottky Solar Cells Based on Colloidal Nanocrystal Films. *Nano Lett.* **2008**, *8*, 3488–3492.
4. Colvin, V.; Schlamp, M.; Alivisatos, A. Light-Emitting Diodes Made from Cadmium Selenide Nanocrystals and a Semiconducting Polymer. *Nature* **1994**, *370*, 354–357.
5. Klimov, V.; Mikhailovsky, A.; Xu, S.; Malko, A.; Hollingsworth, J.; Leatherdale, C.; Eisler, H.-J.; Bawendi, M. Optical Gain and Stimulated Emission in Nanocrystal Quantum Dots. *Science* **2000**, *290*, 314–317.
6. Royne, A.; Dey, C. J.; Mills, D. R. Cooling of Photovoltaic Cells under Concentrated Illumination: A Critical Review. *Sol. Energy Mater. Sol. Cells* **2005**, *86*, 451–483.
7. Buso, S.; Spiazzi, G.; Meneghini, M.; Meneghesso, G. Performance Degradation of High-Brightness Light Emitting Diodes Under DC and Pulsed Bias. *IEEE Trans. Device Mater. Reliab.* **2008**, *8*, 312–322.
8. Braithwaite, J.; Silver, M.; Wilkinson, V.; O'Reilly, E.; Adams, A. Role of Radiative and Nonradiative Processes on the Temperature Sensitivity of Strained and Unstrained 1.5 μm InGaAs (P) Quantum Well Lasers. *Appl. Phys. Lett.* **1995**, *67*, 3546–3548.
9. Pugh-Thomas, D.; Walsh, B. M.; Gupta, M. C. CdSe(ZnS) Nanocomposite Luminescent High Temperature Sensor. *Nanotechnology* **2011**, *22*, 185503.
10. Rowland, C. E.; Schaller, R. D. Exciton Fate in Semiconductor Nanomaterials at Elevated Temperatures: Hole Trapping Out-Competes Exciton Deactivation. *J. Phys. Chem. C* **2013**, *117*, 17337–17343.

11. Rowland, C. E.; Liu, W.; Hannah, D. C.; Chan, M. K. Y.; Talapin, D. V.; Schaller, R. D. Thermal Stability of Colloidal InP Nanocrystals: Small Inorganic Ligands Boost High-Temperature Photoluminescence. *ACS Nano* **2014**, *8*, 977–985.
12. Zhao, Y.; Riemersma, C.; Pietra, F.; Koole, R.; de Mello Donegá, C.; Meijerink, A. High-Temperature Luminescence Quenching of Colloidal Quantum Dots. *ACS Nano* **2012**, *6*, 9058–9067.
13. Narayanaswamy, A.; Feiner, L. F.; Meijerink, A.; van der Zaag, P. J. The Effect of Temperature and Dot Size on the Spectral Properties of Colloidal InP/ZnS Core−Shell Quantum Dots. *ACS Nano* **2009**, *3*, 2539–2546.
14. Cai, X.; Martin, J. E.; Shea-Rohwer, L. E.; Gong, K.; Kelley, D. F. Thermal Quenching Mechanisms in II−VI Semiconductor Nanocrystals. *J. Phys. Chem. C* **2013**, *117*, 7902–7913.
15. Porter, V. J.; Geyer, S.; Halpert, J. E.; Kastner, M. A.; Bawendi, M. G. Photoconduction in Annealed and Chemically Treated CdSe/ZnS Inorganic Nanocrystal Films. *J. Phys. Chem. C* **2008**, *112*, 2308–2316.
16. Gelloz, B.; Sano, H.; Boukherroub, R.; Wayner, D. D. M.; Lockwood, D. J.; Koshida, N. Stabilization of Porous Silicon Electroluminescence by Surface Passivation with Controlled Covalent Bonds. *Appl. Phys. Lett.* **2003**, *83*, 2342–2344.
17. Mangolini, L.; Kortshagen, U. Plasma-Assisted Synthesis of Silicon Nanocrystal Inks. *Adv. Mater.* **2007**, *19*, 2513–2519.
18. Goldstein, A. N. The Melting of Silicon Nanocrystals: Submicron Thin-Film Structures Derived from Nanocrystal Precursors. *Appl. Phys. A: Mater. Sci. Process.* **1996**, *62*, 33–37.
19. Hirasawa, M.; Orii, T.; Seto, T. Size-Dependent Crystallization of Si Nanoparticles. *Appl. Phys. Lett.* **2006**, *88*, 093119.
20. Lu, H. M.; Li, P. Y.; Cao, Z. H.; Meng, X. K. Size-, Shape-, and Dimensionality-Dependent Melting Temperatures of Nanocrystals. *J. Phys. Chem. C* **2009**, *113*, 7598–7602.
21. Biju, V.; Makita, Y.; Sonoda, A.; Yokoyama, H.; Baba, Y.; Ishikawa, M. Temperature-Sensitive Photoluminescence of CdSe Quantum Dot Clusters. *J. Phys. Chem. B* **2005**, *109*, 13899–13905.
22. Van Sickle, A. R.; Miller, J. B.; Moore, C.; Anthony, R. J.; Kortshagen, U. R.; Hobbie, E. K. Temperature Dependent Photoluminescence of Size-Purified Silicon Nanocrystals. *ACS Appl. Mater. Interfaces* **2013**, *5*, 4233–8.
23. de Mello Donegá, C.; Bode, M.; Meijerink, A. Size- and Temperature-Dependence of Exciton Lifetimes in CdSe Quantum Dots. *Phys. Rev. B* **2006**, *74*.
24. Crooker, S. A.; Barrick, T.; Hollingsworth, J. A.; Klimov, V. I. Multiple Temperature Regimes of Radiative Decay in CdSe Nanocrystal Quantum Dots: Intrinsic Limits to the Dark-Exciton Lifetime. *Appl. Phys. Lett.* **2003**, *82*, 2793–2795.
25. Wautelet, M. Estimation of the Variation of the Melting Temperature with the Size of Small Particles, on the Basis of a Surface-Phonon Instability Model. *J. Phys. D: Appl. Phys.* **1991**, *24*, 343.
26. Varshni, Y. P. Temperature Dependence of the Energy Gap in Semiconductors. *Physica* **1967**, *34*, 149–154.
27. Farrell, H. H.; Van Siclen, C. D. Binding Energy, Vapor Pressure, and Melting Point of Semiconductor Nanoparticles. *J. Vac. Sci. Technol., B* **2007**, *25*, 1441–1447.
28. Shi, F. G. Size Dependent Thermal Vibrations and Melting in Nanocrystals. *J. Mater. Res.* **1994**, *9*, 1307–1314.
29. Hong, S.; Chou, M. Y. Effect of Hydrogen on the Surface-Energy Anisotropy of Diamond and Silicon. *Phys. Rev. B* **1998**, *57*, 6262–6265.
30. Schall, J. D.; Gao, G.; Harrison, J. A. Elastic Constants of Silicon Materials Calculated as a Function of Temperature Using a Parametrization of the Second-Generation Reactive Empirical Bond-Order Potential. *Phys. Rev. B* **2008**, *77*, 115209.
31. Ramana Murty, M. V.; Atwater, H. A. Empirical Interatomic Potential for Si-H Interactions. *Phys. Rev. B* **1995**, *51*, 4889–4893.
32. Gale, J. D.; Rohl, A. L. The General Utility Lattice Program (GULP). *Mol. Simul.* **2003**, *29*, 291–341.
33. Kuan-Chuan, F.; Cheng, I. W. An Investigation into the Melting of Silicon Nanoclusters Using Molecular Dynamics Simulations. *Nanotechnology* **2005**, *16*, 250.
34. Erhart, P.; Albe, K. Analytical Potential for Atomistic Simulations of Silicon, Carbon, and Silicon Carbide. *Phys. Rev. B* **2005**, *71*, 035211.
35. Walsh, R. Bond Dissociation Energy Values in Silicon-Containing Compounds and Some of their Implications. *Acc. Chem. Res.* **1981**, *14*, 246–252.
36. Dohnalová, K.; Gregorkiewicz, T.; Kusová, K. Silicon Quantum Dots: Surface Matters. *J. Phys.: Condens. Matter* **2014**, *26*, 173201.
37. Fan, J. Y.; Wu, X. L.; Chu, P. K. Low-Dimensional SiC Nanostructures: Fabrication, Luminescence, and Electrical Properties. *Prog. Mater. Sci.* **2006**, *51*, 983–1031.
38. Hannah, D. C.; Yang, J.; Podsiadlo, P.; Chan, M. K. Y.; Demortière, A.; Gosztola, D. J.; Prakapenka, V. B.; Schatz, G. C.; Kortshagen, U.; Schaller, R. D. On the Origin of Photoluminescence in Silicon Nanocrystals: Pressure-Dependent Structural and Optical Studies. *Nano Lett.* **2012**, *12*, 4200–4205.